Available online at www.sciencedirect.com

ScienceDirect

Proceedings of the Combustion Institute 000 (2020) 1–9

Proceedings of the Combustion Institute

www.elsevier.com/locate/proci

Application of chemical graph theory to PAH isomer enumeration and structure in laser desorption/ionization mass spectrometry studies of particulate from an ethylene diffusion flame ☆

J. Houston Miller*, Rachelle J. Golden, Jennifer A. Giaccai, Andrew Kamischke, Andrew Korte, Akos Vertes

Department of Chemistry, The George Washington University, 800 22nd Street, NW, Suite 4000, Washington, DC 20052, United States

Received 7 November 2019; accepted 28 June 2020
Available online xxx

Abstract

Our laboratory recently published data that showed that the PAH composition of soot can be exactly determined and spatially resolved by low-fluence laser desorption ionization, coupled with high-resolution mass spectrometry imaging [1]. This analysis revealed that PAHs of 239–838 Da, containing few oxygenated species, comprise the soot observed in an ethylene diffusion flame. In this paper, we demonstrate that the empirical formula of observed species can aid in the enumeration of isomers and places limits on their structures and thermodynamic stability. Specifically, chemical graph theory (CGT) shows that the vast majority of species observed in the sampled particulate matter may be described as benzenoid, consisting of only fused 6-membered rings. We apply CGT to determine the Dias Parameter, d_S, for observed, individual PAH peaks and demonstrate that observed PAH species cluster near low d_S, indicative of highly condensed structures, with relatively low populations of edge concavity (armchairs, bays, and fjords). Finally, we quantitatively explore the relative stability of PAH isomers using group-additivity estimates (for benzenoid structures) and those containing a single 5-membered rings using density functional theory. For the latter, we show that highly-condensed, benzenoid structures have lower free energy than those containing five-membered rings, with buried 5-membered rings showing the highest free energies.

Keywords: Soot; Polynuclear aromatic hydrocarbons; Graph theory

1. Introduction

A leading hypothesis for the structure of soot particles is that polynuclear aromatic hydrocarbon (PAH) molecules are their dominant components,

☆ Colloquium: Soot, Nanomaterials, and Large Molecules.

* Corresponding author.
E-mail address: houston@gwu.edu (J.H. Miller).

https://doi.org/10.1016/j.proci.2020.06.080

Please cite this article as: J.H. Miller, R.J. Golden and J.A. Giaccai et al., Application of chemical graph theory to PAH isomer enumeration and structure in laser desorption/ionization mass spectrometry studies of particulate from an ethylene diffusion flame, Proceedings of the Combustion Institute, https://doi.org/10.1016/j.proci.2020.06.080

with individual PAH molecules forming ordered stacks that agglomerate into primary particles. In a recent publication, we applied laser desorption and ionization mass spectrometry to the analysis of carbon particulate thermophoretically sampled from a nitrogen-diluted, ethylene/air diffusion flame previously [1]. The mass spectra and subsequent analysis revealed that the particulate is comprised predominately of medium (~300–800 Da), highly condensed structures and their average mass agreed well with our prior experimental determination of "conjugation length" from Raman scattering [2] and optical band gap measurements [3]. As shown in that contribution, an approach for developing structural insight about the PAH comprising the collected particulate is available from chemical graph theory (CGT). In this paper, we analyze these results using tools developed by the applied mathematics community and further explore isomeric variations for thermodynamic stability.

The new analysis builds on the work of Dias [4],[5] and Cyvin [6] who have made extensive contributions to the application of CGT to the enumeration of possible isomeric structures given an empirical formula. Using the mathematical tools developed in the references cited above, important limits emerge to confine the structure of molecules observed in our mass spectrometry experiments. As an example, we had considered one of the mass spectra collected in the wings of the flame. In this spectrum, there are approximately 180 identified m/z peaks (with intensities between 4200 and 86,000). The vast majority of these have empirical formulae consistent with benzenoid hydrocarbons. Specifically, for a hydrocarbon of formula C_nH_s, benzenoid species, those with only 6-membered rings, will satisfy

$$2\left\{\frac{1}{2}\left(n+\sqrt{6n}\right)\right\}-n\le s\le n+2-2\left\{\frac{1}{4}(n-2)\right\}. \quad (1)$$

where quantities within the curly brackets are rounded up to the nearest integer. (We consider the implications of the inclusion of five-membered ring structures in the discussion to follow).

Brunvoll and Cyvin [6] provide a number of additional limitations on and insights into structures based solely on empirical formula. For example, relationships are drawn for the number of internal carbon atoms, $\boldsymbol{n_i}$; the number of hexagonal rings, $\boldsymbol{h}$; and the numbers of isomers, both Kekuléan (closed shell) and non-Kekuléan (radicals). Finally, they provide an extensive discussion on what they refer to as the Dias Parameter, $\boldsymbol{d_s}$, suggested by Dias to be a count of tree disconnections where "trees" are constructed from lines connecting internal carbon atoms. Brunvoll and Cyvin [6] show how the $\boldsymbol{d_s}$ can be calculated directly from the empirical formula C_nH_s from

$$d_s=\frac{1}{2}(3s-n)-7 \quad (2)$$

The Dias Parameter is 0 when there are no disconnections, positive when there are, and negative for branched trees which occur when there are extensive networks of interior carbons. As an example, consider several 6-ring molecules which were observed in our mass spectra: $C_{24}H_{12}$ (coronene), $C_{25}H_{13}$, $C_{26}H_{14}$, $C_{27}H_{15}$. All the isomers of the odd-carbon species are radicals (as well as a small number of the isomers of the even-carbon species). The number of possible isomers (1, 3, 10, and 5, respectively [6]) grows with $\boldsymbol{d_s}$ (−1, 0, 1, and 2) while it is observed that the MS intensity is greater for the low $\boldsymbol{d_s}$ molecules (10,365, 26,997, 5226, and 8558, respectively) despite the statistically smaller number of structures that satisfy the empirical formula for low $\boldsymbol{d_s}$. The same trends are seen for groups containing higher numbers of rings observed in our spectra, as shown in Fig. 2.

2. Description of experimental procedures and data

A report of the experimental procedure has appeared previously [1], [7],[8], and is summarized here. Additional experimental details are provided in the Supplemental Materials. The flame studied was a nitrogen-diluted, ethylene-air flames (60% ethylene by volume) supported on a burner developed at Yale University. It has been extensively studied and modelled by our laboratory and our collaborators at Yale [2],[9–17]. Additionally, it is a target, non-premixed flame of the International Sooting Flame workshop because of its established dilution levels that span a range of sooting levels and residency times. The burner consists of a central fuel tube with an inner diameter of 0.4 cm and a concentric air co-flow tube with an inner diameter of 5.1 cm. A stable flame is maintained using co-flowing air emitted from a honeycomb [10],[17].

All measurements were made on a Thermo LTQ MALDI-LTQ-Orbitrap XL mass spectrometer (Thermo Scientific, San Jose, CA). This instrument is equipped with an intermediate-pressure (75 mTorr) commercial MALDI source, which includes a nitrogen laser emitting 337 nm light with 4 ns pulse width and a repetition rate of 60 Hz. Silicon and aluminum sample substrates were affixed to a commercial sample plate using double-sided carbon tape (Ted Pella, Inc., Redding, CA) before insertion into the source. The carbon tape has not been shown to result in spectral features unless directly exposed to laser radiation. All spectra were acquired in the Orbitrap analyzer with nominal mass resolution set to 60,000.

Particulate from the flame was thermophoretically sampled onto low resistivity p-type silicon wafers (Silicon Valley Microelectronics, Inc., Santa

Please cite this article as: J.H. Miller, R.J. Golden and J.A. Giaccai et al., Application of chemical graph theory to PAH isomer enumeration and structure in laser desorption/ionization mass spectrometry studies of particulate from an ethylene diffusion flame, Proceedings of the Combustion Institute, https://doi.org/10.1016/j.proci.2020.06.080

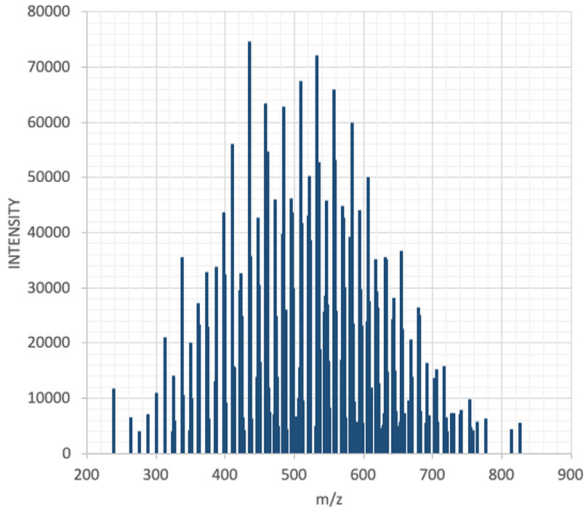

Fig. 1. Representative LDI-MS data from 30 mm above the burner in the flame wing.

Clara, CA). The substrates were inserted into the center of the axially symmetric flame, and the resulting deposition pattern provided a map of soot composition that may be compared with radial distribution of molecular and condensed-phase species measured by other techniques. After sampling, the wafers were analyzed by laser desorption ionization (LDI)-mass spectrometry (MS) imaging with a mass spectrometer capable of high mass resolution and accurate mass measurements.

When samples were introduced into this instrument, a camera takes a visible image of the surface so that the area of analysis can be selected by the user. In these imaging experiments, the laser power was adjusted for each measurement. One image pixel was an average of four scans, taken at four adjacent areas; each scan was acquired with 10 laser shots and separated by 100 μm in physical space on the sample surface, with the next pixel centered 200 μm over. Pixels were obtained in a raster pattern. All measurements reported were the average of 49 total scans.

Initial data processing is done using Xcalibur QualBrowser software (Thermo Scientific, San Jose, CA). Spectra were averaged, and the resulting averaged spectrum lists were exported to mMass version 5.5, an open source software tool [18]. A homebuilt library was constructed in Python (v. 2.7) consisting of all possible molecular combinations weighing less than 2000 Da of 150 carbons, 150 hydrogens, and 4 oxygens, without accounting for the stability of the resulting molecule. It is well known that the availability and number of various elements has a significant impact on peak identification; a specific m/z value could correspond very closely with a PAH of 56 carbons, but if the library is limited to 50 carbons, a similar m/z may be achieved with 38 carbons and 13 oxygens, regardless of the practical likelihood of oxygenation.

There is an extensive literature available on the analysis of PAH, including their determination in environmental samples, including water and soil, or food products. (Many PAHs are tightly regulated by the Environmental Protection Agency due to their known carcinogenic effects [19].) Mass spectrometric techniques are used extensively to analyze more complex mixtures of larger PAHs from raw fuel materials, a field known as petroleomics. The main limitation of LDI is that there is an inherent requirement that the sample efficiently absorb the incident wavelength. PAH molecules are broadly absorbing and are ionized efficiently by UV radiation. As a consequence, molecular complexes (e.g. dimers, trimers, etc.) or fragmentation is often observed upon ionization. To explore the possibility for artifacts introduced in the experiments, a series of experiments were performed on pure coronene or a PAH standard mixture. (See Supplemental Materials). Finally, it is not uncommon to observe the formation of carbon clusters, or more specifically fullerenes, in mass spectra of carbon rich material upon laser absorption [20],[21]. In our studies, under the lowest fluence conditions, there were no clusters of carbon observed in the mass spectrum. Importantly, when the laser fluence was increased, there were many carbon cluster ions observed even when coronene was the only primary analyte.

A representative mass spectrum for a region 30 mm above the burner and in the soot "wing" area is shown in Fig. 1. Our PAH distribution is centered at higher mass values than previously reported MBMS or early LMMS results. In addition to the sampling method, the two most significant

Please cite this article as: J.H. Miller, R.J. Golden and J.A. Giaccai et al., Application of chemical graph theory to PAH isomer enumeration and structure in laser desorption/ionization mass spectrometry studies of particulate from an ethylene diffusion flame, Proceedings of the Combustion Institute, https://doi.org/10.1016/j.proci.2020.06.080

differences between the current study and others are the low laser fluence (3.2 mJ/cm^2) combined with a more sensitive, and higher-resolution imaging mass spectrometer. The high mass resolving power of the Orbitrap analyzer allows for the resolution of nearly-isobaric species. This, combined with accurate m/z measurements improved by internal calibration to previously identified PAH ions, allows for the confident assignment of molecular formulae.

In the observed data, the flame areas of maximum mass spectrometric intensity was positioned between the region rich in hydrocarbon intermediates formed directly from fuel ethylene decomposition [22] and the high-temperature, radical rich region height [2].

3. Isomer enumeration and thermodynamic analysis

3.1. Generation of molecular structures from graph theory

The *Chemical and abstract Graph environment* (CaGe) program is an open-source software tool that applies graph theory to molecular structures [23]. CaGe's molecular generator enumerates *graphs* that serve as models for molecules. *Graphs* consist of *vertices* (or nodes) and *edges* (or connections) with adjacent vertices connected by an edge. The number of edges starting at a vertex (or the number of adjacent vertices) is the *valency* (or *degree*) of that vertex.

The *hydrocarbon* generator in CaGe package creates graphs consisting of planar (or near planar) structures with pentagonal and hexagonal faces. In the language of CGT, for 2-connected plane graphs with a distinguished outer face where all bounded faces are pentagons or hexagons, all vertices not in the boundary of the outer face have degree 3 and all vertices in the boundary of the outer face have degree 2 or 3. In the more familiar language of carbon-bonding, the working assumption is that all carbons in the structure are sp^2 hybridized and the degree can be used to distinguish edge from interior carbons. Further, by generating the entire suite of isomers characteristic of a given empirical formula, an inventory of edge-carbon morphology can be developed that will distinguish "zig zag", "armchair", "bay", and "fjord" sites, as shown below.

3.2. Thermodynamic stability and equilibrium calculations

The enumeration of isomeric structures using CaGe software produces a mapping of atomic connectivity, but does not produce optimized chemical structures and thus does not provide quantitative insight into thermodynamic stability. After the structures of the possible isomers were generated by CaGe software, adjacency lists were created using our own python program. The initial focus was on hexagonal, completely benzenoid structure. To determine the thermodynamic stability of different isomers, the group additivity approach developed by Yu was used [24], which can be accessed using the thermodynamic part of the Reaction Mechanism Generator (RMG) Python package or the RMG website produced by the Green group at MIT and West group at Northeastern University [25].

The thermodynamic libraries generated by RMG contained the NASA polynomials for each isomer CaGe constructed. For a family of PAH structures with a fixed number of aromatic rings, a gas mixture was constructed by adding these to the GRI 3.0 mechanism [26] and was solved for their equilibrium concentrations at a given temperature and pressure using the chemical equilibria solver of Cantera [27]. These calculations were done for 7-, 8-, 9-, and 10-ring PAH families. The starting elemental concentrations for carbon and hydrogen were set to match PAH with the greatest H/C ratio. These calculations were run every 100 K from 1500 to 2000 K and 1 atm. for each set.

When molecules containing 5-membered rings were evaluated, all bonds needed to be explicitly determined as the CaGe program would often produce non-Kekulean isomeric structures. For these isomers as well as ovalene, thermodynamic properties were evaluated by using density functional theory (DFT) in the NWChem computational chemistry program version 6.5 [28],[29]. Molecules were first geometry optimized using the 6–31G* basis set and the B3LYP exchange-correlation functional before frequency calculations were carried out using the 6–311G* basis set every 100 K between 300 and 2200 K. This basis set and functional have been shown to provide acceptable resolution for geometry optimization for PAH [30],[31]. Although this level of theory will not produce quantitatively accurate thermodynamics values, our goal here was only to compare relative magnitudes between structurally similar molecules. Specifically, we were interested in the equilibrium between single 5-membered-ring-containing isomers of $C_{32}H_{14}$ (abbreviated below as 1_5_XX, where XX is s structural index generated by CaGe code) and ovalene.

$$1\_5\_XX \rightleftarrows Ovalene \tag{R.1}$$

$$\Delta G = (\varepsilon_0 + G_{corr})_{product} - (\varepsilon_0 + G_{corr})_{reactant} \tag{3}$$

Where ε_0 is the zero-point energy of the DFT calculation and G_{corr} is given by quantities generated in the NWCHEM vibrational analysis through

$$G_{corr} = H_{corr} - T \cdot S_{tot} \tag{4}$$

Please cite this article as: J.H. Miller, R.J. Golden and J.A. Giaccai et al., Application of chemical graph theory to PAH isomer enumeration and structure in laser desorption/ionization mass spectrometry studies of particulate from an ethylene diffusion flame, Proceedings of the Combustion Institute, https://doi.org/10.1016/j.proci.2020.06.080

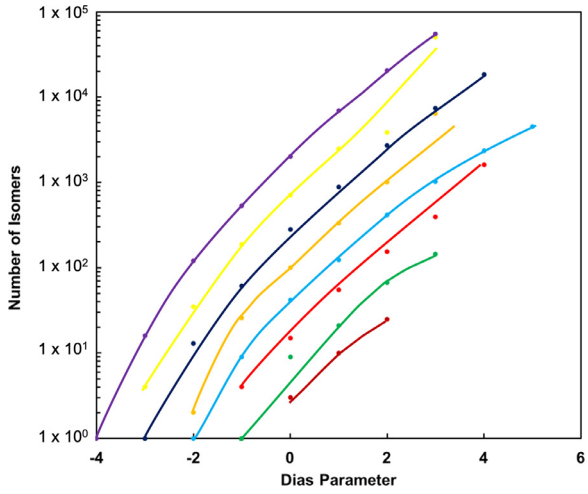

Fig. 2. ***CaGe*** predictions of the number of isomers as a function of ring count and d_s for observed LDI-MS peaks. Color Key: orange-7 rings, aqua-8 rings, red-9 rings, blue-10 rings, dark yellow-11 rings, dark blue-12 rings, yellow-13 rings, purple-14 rings. (For interpretation of the references to color in this figure legend, the reader is referred to the web version of this article.)

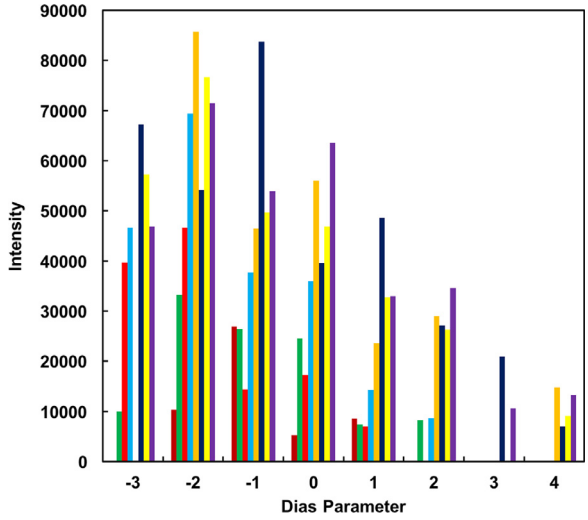

Fig. 3. Observed peak intensities for a range of ring counts sorted by d_s. See Fig. 2 for color scale.

4. Computational results and discussion

4.1. Isomer enumeration and observed structural trends

As noted in the introduction, the number of possible isomers increases rapidly with d_S and identifying molecular structural trends within this data is a daunting task, one that is only enabled through the use of ***CaGe***. Shown in Fig. 2 is the exponential increase in isomer count for the observed 7–14 ring compounds. Some observations are immediately obvious in this data. First, the range in d_S expands with ring count, h. Second, for either a given d_S or a given ring count, the number of isomers grows exponentially. Third, for the lowest possible d_S in a given ring count family the number of isomers of even-numbered ring counts is one, for odd-numbered ring counts the number of isomers is in the single digits.

Fig. 3 provides insight into the observed distribution of these isomeric species as a function of d_S. As seen in Fig. 2 the number of possible isomers increases with d_s while it is observed that the LDI-MS intensity is greater for the low d_s molecules despite the statistically smaller number of structures

Please cite this article as: J.H. Miller, R.J. Golden and J.A. Giaccai et al., Application of chemical graph theory to PAH isomer enumeration and structure in laser desorption/ionization mass spectrometry studies of particulate from an ethylene diffusion flame, Proceedings of the Combustion Institute, https://doi.org/10.1016/j.proci.2020.06.080

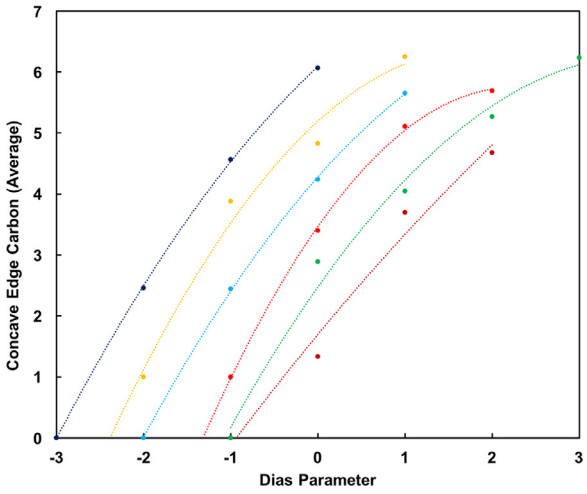

Fig. 4. Number of concave edge carbons for a range of ring counts sorted by d_s. See Fig. 2 for color scale.

that satisfy the empirical formula for low d_s. As discussed below, this is an important observation with implications for thermodynamic stability of the chemical components of incipient particles.

For likely PAH structures observed in flames, it is expected that as the d_s is increased, the number of interior carbons and the extent of aromatic conjugation must both decrease. To explore this hypothesis, ***CaGe*** was used to identify structures for (in some cases thousands of) isomers for a given ring count and d_s. This was accomplished by counting the number of non-zigzag, concave edge carbons found in the armchair, bay, and fjord regions in a given structure. These counts were then averaged to determine the number of concave edge carbons noting that an armchair represents two edge carbons, a bay three, and a fjord four. The result of this procedure is shown in Fig. 4 for each observed peak in the mass spectrum shown in Fig. 1. As anticipated, increasing d_s leads to an increase in the count of concave edge carbons. Further, this effect is more pronounced with increasing ring count.

4.2. Implications for thermodynamic stability

In a recent publication from our group, we showed how the Clar model, a method of studying the aromaticity of a structure, could be applied to an understanding of thermodynamic stability for different PAH isomers [32]. In Clar structures, the π electrons in a polycyclic ring structure are assigned so that the maximum number of rings has 6 π electrons, known as an aromatic sextet [33]. The Clar structure approach to understanding molecular structure has been validated by both atomic force microscopy and scanning tunneling microscopy [34]. The kinetic and thermodynamic stability of isomers increases with an increase in number of aromatic sextets because of additional resonance energy [33].

The evaluation of resonant energy in large PAH has found increased focus as these molecules are thought to be ideal model systems for the understanding of bonding and electronic structure in nanographene compounds [35]. It has been found that the nature of PAH edges has a profound effect on the number of Clar sextets that may exist for a PAH isomer and thus electronic structure and thermodynamic stability. It is worth noting that counting sextets for irregularly shaped, large PAH can be challenging [36], and new measures of stability have been introduced, including bond resonance energy (BRE) and superaromatic stabilization energy (SSE). SSE is defined as the extra stabilization energy due to macrocyclic conjugation in these large π-systems, and thus is manifested in interior regions of large PAH. Specifically, Dias notes that for benzocoronenes, in the peripheral hexagons BRE = SSE, but for inner hexagons BRE > SSE [37]. In this work, we note that additional resonance stabilization for interior carbons will be more relevant for structures with the most extensive network of interior conjugation, structures with minimal d_s.

Clearly, the presence of non-zigzag carbon features on the periphery of aromatic structures decreases the size of these superaromatic regimes and thus the thermodynamic stability of a particular isomer. Further, the presence of fjords in a molecule further decrease stability due to the steric interference of hydrogen atoms within the edge cavity leading to non-planar structures. The fact that the LDI-MS data clusters near low d_s suggests that the PAH components of soot are these most stable structures and are dominated by planar, hexagonal networks. This conjecture is explored quantitatively in the next section.

Please cite this article as: J.H. Miller, R.J. Golden and J.A. Giaccai et al., Application of chemical graph theory to PAH isomer enumeration and structure in laser desorption/ionization mass spectrometry studies of particulate from an ethylene diffusion flame, Proceedings of the Combustion Institute, https://doi.org/10.1016/j.proci.2020.06.080

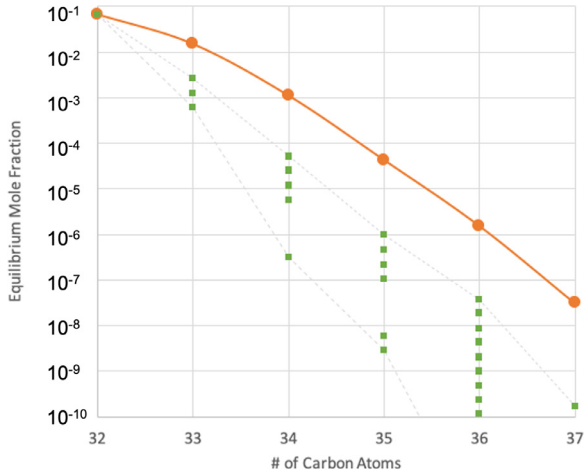

Fig. 5. Equilibrium mole fractions of 10-ring PAH at 1500 K and 1 atm. Total concentration are the orange circles and individual isomers are the green squares. (For interpretation of the references to color in this figure legend, the reader is referred to the web version of this article.)

4.2.1. Thermodynamic stability of benzenoid PAH

In the mid 1980s Stein and Fahr [38] showed that certain isomers of PAH were the most thermodynamically stable isomeric form for given inventories of carbon and hydrogen atoms and these were labeled as stabilomers. It is important to note that although the original stabilomer study included only PAH with even numbers of carbon atoms, benzenoid structures can be comprised of an odd number of carbons, e.g., $C_{13}H_9$, $C_{47}H_{17}$ [39]. The initial Stein and Fahr work, and many follow-on studies used group additivity methods to estimate thermodynamics properties for these species. The Green group of MIT has greatly improved on the older group additivity estimates for PAH by adding an algorithm for bicyclic decomposition for large (>3 rings) PAH species [40].

Fig. 5 shows equilibrium mole fractions for 10-ring, benzenoid PAH at 1500 K and 1 atm as described in Section 3.2. Similar trends were observed for temperatures between 1500 and 2000 K. A total of 8467 unique isomers of these 10-ring PAH were included in this equilibrium mixture ranging from 32 to 39 carbon atoms. (For this family of PAH, #H =#C-18. Further, via Eq. (2) we see that $\boldsymbol{d_s}$ = #C-34). As shown in Fig. 2, the number of isomers increases rapidly with $\boldsymbol{d_s}$. However, RMG predicted a range of thermodynamic stability among molecules with the same $\boldsymbol{d_s}$. As the complexity of PAH structures increased (towards larger $\boldsymbol{d_s}$), degeneracies within these subsets also increased. For example, for $C_{33}H_{15}$, there are 9 unique isomeric structures that are predicted to have one of three values for free energy at 1500 K and thus three equilibrium mole fractions, shown as green squares in Fig. 5. The orange circle at each #C gives the sum of all isomeric concentrations for that empirical formula. In agreement with the observed LDI-MS peak intensities (Fig. 3), for these 10-ring PAH the lower $\boldsymbol{d_s}$ species are predicted to be the most thermodynamically stable. The same trend is observed for PAH with higher and lower ring counts.

4.2.2. Comparative stability for $C_{32}H_{14}$ PAH containing one 5-membered ring

As reviewed in the earlier report of the measurements described here [1], recent literature suggests the importance of PAH structures which include five-membered rings [41–43]. Addition of even one pentagon into a PAH structure (fluoranthenoids) dramatically increases the number of possible isomers and, fortunately, these may also be enumerated using CaGe. Here, we concentrate on a subset of 10-ring PAH isomers of $C_{32}H_{14}$ including ovalene, shown above to be the most stable benzenoid structure, and six of the 75 isomers that contain one 5-membered rings of the same empirical formula. Two of the structures have buried pentagons leading to bowl shaped geometries, two have edge pentagons that include one C–H bond, and two have edge pentagons that contain two C–H bonds. (Structures for these species are included in the Supplementary Material). In our previous paper [1], we showed that inclusion of 5-membered rings increases sigma character and leads to greater reactivity of interior carbons.

For the examples studied at 1500 K we found that ovalene remained the most stable of the $C_{32}H_{14}$ isomers, with structures with edge 5-membered rings with two C–H groups next (ΔG of R1 = −30±0 kcal/mol), followed by edge 5-membered rings with one C–H groups (−41±0 kcal/mol), and finally structures with buried 5-membered rings (−65±7 kcal/mol). These

Please cite this article as: J.H. Miller, R.J. Golden and J.A. Giaccai et al., Application of chemical graph theory to PAH isomer enumeration and structure in laser desorption/ionization mass spectrometry studies of particulate from an ethylene diffusion flame, Proceedings of the Combustion Institute, https://doi.org/10.1016/j.proci.2020.06.080

results highlight the fact that the bowl-shaped molecules with pentagons occurring in the interior of the PAH molecule are the least preferred isomers, when compared to ovalene or the isomers with pentagons occurring on the edge of the molecule.

5. Conclusions

In this paper, we extend the analysis of recently published results of low-fluence, high-resolution, imaging LDI-MS in which we suggested that benzenoid PAH molecules are the building blocks of soot particles. From observed empirical formulae, we show that chemical graph theory can be used to determine important structural parameters and lead to both isomer enumeration and to inventory edge carbon topology. Further, through the application of both group additivity techniques and thermodynamic analysis vis DFT computational chemistry, we show that the PAH observed in soot tend towards highly condensed and thermodynamically stable structures.

These new results illuminate an ongoing debate in the chemical growth community: are there sufficiently high concentrations of large monomer PAH in flames to explain observed primary particle concentrations? Although we raised this concern in an early calculation of the equilibrium constant for the dimerization constant for PAH [44], in subsequent publications, we qualified this conclusion by noting that sufficiently large PAH will physically condense at temperatures characteristic of soot formation in diffusion flames [45], and this conclusion has been supported by recent molecular dynamics simulations of both physical and chemical condensation [46],[47]. The new LDI-MS results and the analysis reported here provide evidence that species of sufficient size are present within carbon particulates in flames and that their size is consistent with the conjugation length inferred by both Raman scattering and optical band gap measurements observed in the same burner/flame system [2],[3]. What remains to be determined is how these PAH came to be there, either through more complex chemistry in the gas phase [48–51],[52],[53], or graphitization within the growing particles.

Declaration of Competing Interest

The authors declare that they have no known competing financial interests or personal relationships that could have appeared to influence the work reported in this paper.

Acknowledgments

This material is based upon work supported by the U.S. National Science Foundation under grant number CBET- 1706757 with Drs. Song-Charng Kong and Harsha Chelliah serving as technical monitors.

Supplementary materials

Supplementary material associated with this article can be found, in the online version, at doi:10.1016/j.proci.2020.06.080.

References

[1] R.S. Jacobson, A.R. Korte, A. Vertes, J.H. Miller, *Angew. Chem. Int. Ed.* 59 (2020) 4484–4490.
[2] J.D. Herdman, B.C. Connelly, M.D. Smooke, M.B. Long, J.H. Miller, *Carbon N.Y.* 49 (2011) 5298–5311.
[3] E.M. Adkins, J.H. Miller, *PCCP* 17 (2015) 2686–2695.
[4] J.R. Dias, *J. Mol. Struct. THEOCHEM* 137 (1986) 9–29.
[5] J. Dias, *Cheminform* (2003) 34.
[6] J. Brunvoll, S. Cyvin, *Z. Naturforschung A* 45 (1990).
[7] R.S. Jacobson, A.R. Korte, A. Vertes, J.H. Miller, *Angdew. Chem. Int. Ed.* (2019) submitted for publication.
[8] R.S.J. Golden, *The Development of Laser-Based Analytical Tools for Molecular Composition Characterization Across Combustion and Biological Systems, Chemistry*, George Washington University, Washington, DC, 2019.
[9] M.D. Smooke, R.J. Hall, M.B. Colket, J. Fielding, M.B. Long, C.S. McEnally, L.D. Pfefferle, *Combust. Theory Model.* 8 (2004) 593–606.
[10] M.D. Smooke, M.B. Long, B.C. Connelly, M.B. Colket, R.J. Hall, *Combust. Flame* 143 (2005) 613–628.
[11] S.A.K. Blair C Connelly, M.D Smooke, M.B Long, *Proc. US Sect. Combust. Inst.* 4 (2005).
[12] S.B. Dworkin, M.D. Smooke, V. Giovangigli, *Proc. Combust. Inst.* 32 (2009) 1165–1172.
[13] M.A. Puccio, J.D. Herdman, J.H. Miller, B.C. Connelly, M.D. Smooke, M.B. Long, *Chem. Phys. Process. Combust.* (2005) 217–220.
[14] B.C. Connelly, B.A. Bennett, S. Dworkin, M.D. Smooke, M.B. Long, M.A. Puccio, J.D. Herdman, J.H. Miller, *Chem. Phys. Process. Combust.* (2005) 259–262.
[15] S.B. Dworkin, B.C. Connelly, A.M. Schaffer, B.A.V. Bennett, M.B. Long, M.D. Smooke, M.P. Puccio, B. McAndrews, J.H. Miller, *Proc. Combust. Inst.* 31 (2007) 971–978.
[16] J.H. Miller, J.D. Herdman, C.D.O. Green, E.M. Webster, *Proc. Combust. Inst.* 34 (2013) 3669–3675.
[17] E.M. Adkins, J.H. Miller, *Phys. Chem. Chem. Phys.* 17 (2015) 2686–2695.
[18] M. Strohalm, M. Hassman, B. Košata, M. Kodíček, *Rapid Commun. Mass Spectrom.* 22 (2008) 905–908.
[19] S.-.S. Cai, J.A. Syage, K.A. Hanold, M.P. Balogh, *Anal. Chem.* 81 (2009) 2123–2128.
[20] H.W. Kroto, A.W. Allaf, S.P. Balm, *Chem. Rev.* 91 (1991) 1213–1235.
[21] H.W. Kroto, J.R. Heath, S.C. O'Brien, R.F. Curl, R.E. Smalley, *Nature* 318 (1985) 162.

Please cite this article as: J.H. Miller, R.J. Golden and J.A. Giaccai et al., Application of chemical graph theory to PAH isomer enumeration and structure in laser desorption/ionization mass spectrometry studies of particulate from an ethylene diffusion flame, Proceedings of the Combustion Institute, https://doi.org/10.1016/j.proci.2020.06.080

[22] K.C. Smyth, J.H. Miller, R.C. Dorfman, W.G. Mallard, R.J. Santoro, *Combust. Flame* 62 (1985) 157–181.
[23] G. Brinkmann, O. Friedrichs, S. Lisken, A. Peeters, N. Van Cleemput, *MATCH Commun. Math. Comput. Chem.* 63 (2010) 533–552.
[24] J. Yu, R. Sumathi, W.H. Green, *J. Phys. Chem. A* 110 (2006) 6971–6977.
[25] C.W. Gao, J.W. Allen, W.H. Green, R.H. West, *Comput. Phys. Commun.* 203 (2016) 212–225.
[26] G.P. Smith, D.M. Golden, M. Frenklach, N.W. Moriarty, B. Eiteneer, M. Goldenberg, C.T. Bowman, R.K. Hanson, S. Song, J. William C. Gardiner, V.V. Lissianski, Z. Qin, GRI-Mech 3.0. http://combustion.berkeley.edu/gri-mech/releases.html 2020).
[27] D. Goodwin, H. Moffat, R. Speth, Cantera: An Object-oriented Software Toolkit for Chemical Kinetics, Thermodynamics, and Transport Processes. Version 2.4.0. https://www.cantera.org, doi:10.5281/zenodo.1174508.
[28] M. Valiev, E.J. Bylaska, N. Govind, K. Kowalski, T.P. Straatsma, H.J.J. Van Dam, D. Wang, J. Nieplocha, E. Apra, T.L. Windus, W.A. de Jong, NWChem, *Comput. Phys. Commun.* 181 (2010) 1477–1489.
[29] E. Aprà, E.J. Bylaska, W.A. de Jong, N. Govind, K. Kowalski, T.P. Straatsma, M. Valiev, H.J.J. van Dam, Y. Alexeev, J. Anchell, V. Anisimov, F.W. Aquino, R. Atta-Fynn, J. Autschbach, N.P. Bauman, J.C. Becca, D.E. Bernholdt, K. Bhaskaran-Nair, S. Bogatko, P. Borowski, J. Boschen, J. Brabec, A. Bruner, E. Cauët, Y. Chen, G.N. Chuev, C.J. Cramer, J. Daily, M.J.O. Deegan, T.H. Dunning, M. Dupuis, K.G. Dyall, G.I. Fann, S.A. Fischer, A. Fonari, H. Früchtl, L. Gagliardi, J. Garza, N. Gawande, S. Ghosh, K. Glaesemann, A.W. Götz, J. Hammond, V. Helms, E.D. Hermes, K. Hirao, S. Hirata, M. Jacquelin, L. Jensen, B.G. Johnson, H. Jónsson, R.A. Kendall, M. Klemm, R. Kobayashi, V. Konkov, S. Krishnamoorthy, M. Krishnan, Z. Lin, R.D. Lins, R.J. Littlefield, A.J. Logsdail, K. Lopata, W. Ma, A.V. Marenich, J. Martin del Campo, D. Mejia-Rodriguez, J.E. Moore, J.M. Mullin, T. Nakajima, D.R. Nascimento, J.A. Nichols, P.J. Nichols, J. Nieplocha, A. Otero-de-la-Roza, B. Palmer, A. Panyala, T. Pirojsirikul, B. Peng, R. Peverati, J. Pittner, L. Pollack, R.M. Richard, P. Sadayappan, G.C. Schatz, W.A. Shelton, D.W. Silverstein, D.M.A. Smith, T.A. Soares, D. Song, M. Swart, H.L. Taylor, G.S. Thomas, V. Tipparaju, D.G. Truhlar, K. Tsemekhman, T. Van Voorhis, Á. Vázquez–Mayagoitia, P. Verma, O. Villa, A. Vishnu, K.D. Vogiatzis, D. Wang, J.H. Weare, M.J. Williamson, T.L. Windus, K. Woliński, A.T. Wong, Q. Wu, C. Yang, Q. Yu, M. Zacharias, Z. Zhang, Y. Zhao, R.J. Harrison, *J. Chem. Phys.* 152 (2020) 184102.
[30] E.M. Adkins, J.A. Giaccai, J.H. Miller, *Proc. Combust. Inst.* 36 (2017) 957–964.
[31] T.C. Allison, D.R. Burgess, *J. Phys. Chem. A* 119 (2015) 11329–11365.
[32] E.M. Adkins, J.H. Miller, *Phys. Chem. Chem. Phys.* 19 (2017) 28458–28469.
[33] E. Clar, R. Schoental, *Polycyclic Hydrocarbons*, Springer, 1964.
[34] M. Solà, *Front. Chem.* 1 (2013) 1–22.
[35] K. Sakamoto, N. Nishina, T. Enoki, J.-I. Aihara, *J. Phys. Chem. A* 118 (2014) 3014–3025.
[36] N. Nishina, M. Makino, J.-i. Aihara, *J. Phys. Chem. A* 120 (2016) 2431–2442.
[37] J.R. Dias, *J. Phys. Chem. A* 123 (2019) 3229–3238.
[38] S.E. Stein, A. Fahr, *J. Phys. Chem.* 89 (1985) 3714–3725.
[39] K.H. Homann, *Angew. Chem. Int. Ed.* 37 (1998) 2434–2451.
[40] K. Han, A. Jamal, C.A. Grambow, Z.J. Buras, W.H. Green, *Int. J. Chem. Kinet.* 50 (2018) 294–303.
[41] N. Hansen, M. Schenk, K. Moshammer, K. Kohse-Höinghaus, *Combust. Flame* 180 (2017) 250–261.
[42] P.J.F. Harris, Z. Liu, K. Suenaga, *J. Phys. Condens. Matter* 20 (2008) 362201.
[43] J.W. Martin, R.I. Slavchov, E.K.Y. Yapp, J. Akroyd, S. Mosbach, M. Kraft, *J. Phys. Chem. C* 121 (2017) 27154–27163.
[44] J.H. Miller, K.C. Smyth, W.G. Mallard, *Symp. Int. Combust.* 20 (1985) 1139–1147.
[45] J.H. Miller, *Symp. Int. Combust.* 23 (1991) 91–98.
[46] P. Elvati, A. Violi, *Fuel* 222 (2018) 307–311.
[47] J.S. Lowe, J.Y.W. Lai, P. Elvati, A. Violi, *Proc. Combust. Inst.* 35 (2015) 1827–1832.
[48] J.H. Miller, *Proc. Combust. Inst.* 30 (2005) 1381–1388.
[49] M. Frenklach, A.M. Mebel, *Phys. Chem. Chem. Phys.* 22 (2020) 5314–5331.
[50] R.A. Krueger, G. Blanquart, *Phys. Chem. Chem. Phys.* 21 (2019) 10325–10335.
[51] G. Vitiello, G. De Falco, F. Picca, M. Commodo, G. D'Errico, P. Minutolo, A. D'Anna, *Combust. Flame* 205 (2019) 286–294.
[52] H. Wang, *Proc. Combust. Inst.* 33 (2011) 41–67.
[53] J.W. Martin, D. Hou, A. Menon, L. Pascazio, J. Akroyd, X. You, M. Kraft, *J. Phys. Chem. C* 123 (2019) 26673–26682.

Please cite this article as: J.H. Miller, R.J. Golden and J.A. Giaccai et al., Application of chemical graph theory to PAH isomer enumeration and structure in laser desorption/ionization mass spectrometry studies of particulate from an ethylene diffusion flame, Proceedings of the Combustion Institute, https://doi.org/10.1016/j.proci.2020.06.080